

Non-linear QCD dynamics in two-photon interactions at high energies

V.P. Gonçalves¹, M.S. Kugeratski², E.R. Cazaroto³, F. Carvalho⁴ and F.S. Navarra³

¹ *Instituto de Física e Matemática, Universidade Federal de Pelotas
Caixa Postal 354, 96010-900, Pelotas, RS, Brazil.*

² *Centro de Engenharia da Mobilidade, Universidade Federal de Santa Catarina,
Campus Universitário, Bairro Bom Retiro 89219-905, Joinville, SC, Brazil.*

³ *Instituto de Física, Universidade de São Paulo, C.P. 66318, 05315-970 São Paulo, SP, Brazil*

⁴ *Departamento de Ciências Exatas e da Terra, Universidade Federal de São Paulo,
Campus Diadema, Rua Prof. Artur Riedel, 275,
Jd. Eldorado, 09972-270, Diadema, SP, Brazil*

The perturbative QCD predicts that the growth of the gluon density at small- x (high energies) should saturate, forming a Color Glass Condensate (CGC), which is described in mean field approximation by the Balitsky-Kovchegov (BK) equation. Assuming that the dipole - dipole cross section can be related with the dipole - proton cross section, we calculate the total $\gamma\gamma$, $\gamma^*\gamma^*$ cross-sections and the real photon structure function $F_2^\gamma(x, Q^2)$ using the recent solution of the BK equation with running coupling constant. We demonstrate that this model is able to describe the LEP data at high energies and provides predictions for the very high energy range which will be probed at future linear colliders. Production of heavy flavors in $\gamma\gamma$ collisions is also studied.

PACS numbers: 12.38.-t, 24.85.+p, 25.30.-c

Keywords: Quantum Chromodynamics, Saturation effects.

The high energy limit of the perturbative QCD is characterized by a center-of-mass energy which is much larger than the hard scales present in the problem. The simplest process where this limit can be studied is the high energy scattering between two heavy quark-antiquark states, *i.e.* the onium-onium scattering. For a sufficiently heavy onium state, high energy scattering is a perturbative process since the onium radius gives the essential scale at which the running coupling α_s is evaluated. In the dipole picture [1], the heavy quark-antiquark pair and the soft gluons in the limit of large number of colors N_c are viewed as a collection of color dipoles. In this case, the cross section can be understood as a product of the number of dipoles in one onium state, the number of dipoles in the other onium state and the basic cross section for dipole-dipole scattering due to two-gluon exchange. At leading order (LO), the cross section grows rapidly with the energy ($\sigma \propto \alpha_s^2 e^{(\alpha_P - 1)Y}$, where $(\alpha_P - 1) = \frac{4\alpha_s N_c}{\pi} \ln 2 \approx 0.5$ and $Y = \ln s/Q^2$) because the LO BFKL equation [2] predicts that the number of dipoles in the light cone wave function grows rapidly with the energy. Several shortcomings are present in this calculation. Firstly, in the leading order calculation the energy scale is arbitrary, which implies that the absolute value to the total cross section is therefore not predictable. Secondly, α_s is not running at LO BFKL. Finally, the power growth with energy violates s -channel unitarity at large rapidities. Consequently, new physical effects should modify the LO BFKL equation at very large s , making the resulting amplitude unitary.

A theoretical possibility to modify this behavior in a way consistent with the unitarity is the idea of parton saturation [3], where non-linear effects associated to high parton density are taken into account. The basic idea is that when the parton density increases (and the scattering amplitude tends to the unitarity limit), the linear description present in the BFKL equation breaks down and one enters the saturation regime. In this regime, the growth of the parton distribution is expected to saturate, forming a Color Glass Condensate (CGC), whose evolution with energy is described by an infinite hierarchy of coupled equations for the correlators of Wilson lines (For recent reviews see [4]). In the mean field approximation, the first equation of this hierarchy decouples and boils down to a single non-linear integro-differential equation: the Balitsky-Kovchegov (BK) equation [3]. In the last years the next-to-leading order corrections to the BK equation were calculated [5–7] through the resummation of $\alpha_s N_f$ contributions to all orders, where N_f is the number of flavours. Such calculation allows one to estimate the soft gluon emission and running coupling corrections to the evolution kernel. The authors have verified that the dominant contributions come from the running coupling corrections, which allow us to determine the scale of the running coupling in the kernel. The solution of the improved BK equation was studied in detail in Ref. [6]. In [8] a global analysis of the small x data for the proton structure function using the improved BK equation was performed (See also Ref. [9]). In contrast to the BK equation at leading logarithmic $\alpha_s \ln(1/x)$ approximation, which fails to describe the HERA data, the inclusion of running coupling effects in the evolution renders the BK equation compatible with them (See also [10–12]).

A reaction which is analogous to the process of scattering of two onia discussed above is the off-shell photon scattering

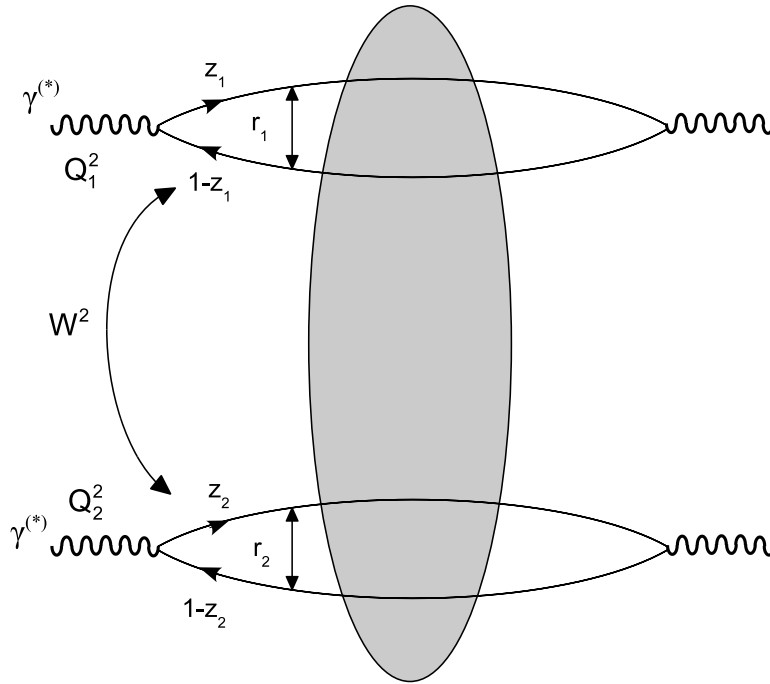


FIG. 1: The diagram illustrating the $\gamma^*\gamma^*$ interaction in the dipole representation. See formula (1).

at high energy in e^+e^- colliders, where the photons are produced from the leptons beams by bremsstrahlung (For a review see, e.g., Ref. [13]). In these two-photon reactions, the photon virtualities can be made large enough to ensure the applicability of the perturbative methods or can be varied in order to test the transition between the soft and hard regimes of the QCD dynamics. From the point of view of the BFKL approach, there are several calculations using the leading logarithmic approximation [14, 15] and considering some of the next-to-leading corrections to the total cross section $\gamma^*\gamma^*$ process [15–18]. On the other hand, the successful description of all inclusive and diffractive deep inelastic data at the collider HERA by saturation models [19–29] suggests that these effects might become important in the energy regime probed by current colliders. This motivated the generalization of the saturation model to two-photon interactions at high energies performed in Ref. [30], which has obtained a very good description of the data on the $\gamma\gamma$ total cross section, on the photon structure function at low x and on the $\gamma^*\gamma^*$ cross section. The formalism used in Ref. [30] is based on the dipole picture [1], with the $\gamma^*\gamma^*$ total cross sections being described by the interaction of two color dipoles, in which the virtual photons fluctuate into (For previous analysis using the dipole picture see, e.g., Refs. [31, 32]). The main assumption in [30], which we also assume as valid, is that the dipole-dipole cross section can be expressed in terms of dipole-proton cross section. In [30] the cross sections were estimated considering the GBW model [19], which is inspired on saturation physics. Although during the last years an intense activity in the area resulted in more sophisticated dipole - proton cross sections [20–29], which could be used to estimate the $\gamma\gamma$ cross sections, the basic consequence of this assumption is that it implies that the dipole-dipole cross section is fully determined by the solution of the BK equation. Consequently, considering the solution provided in [8], we can for the first time estimate the observables in $\gamma\gamma$ collisions using the state-of-the art parametrization of the dipole cross section. In particular, we can provide reliable estimates of the total cross sections and photon structure functions which will be measured in the future linear colliders. This is the main motivation of this paper.

Let us start presenting a brief review of the two-photon interactions in the dipole picture. At high energies, the scattering process can be seen as a succession in time of two factorizable subprocesses (See Fig. 1): i) the photon

fluctuates in quark-antiquark pairs (the dipoles), ii) these color dipoles interact and produce the final state. The corresponding cross section is given by

$$\sigma_{ij}(W^2, Q_1^2, Q_2^2) = \sum_{a,b=1}^{N_f} \int_0^1 dz_1 \int d^2\mathbf{r}_1 |\Psi_i^a(z_1, \mathbf{r}_1)|^2 \int_0^1 dz_2 \int d^2\mathbf{r}_2 |\Psi_j^b(z_2, \mathbf{r}_2)|^2 \sigma_{a,b}^{dd}(\bar{x}_{ab}, r_1, r_2), \quad (1)$$

where the indices i, j label the polarisation states of the virtual photons, i.e. T or L , \mathbf{r} denotes the transverse separation between q and \bar{q} in the color dipole and z is the longitudinal momentum fraction of the quark in the photon. The wave functions $\Psi_i^a(z_k, \mathbf{r})$ are given by

$$|\Psi_i(z, \mathbf{r})|^2 = \sum_f |\Psi_i^f(z, \mathbf{r})|^2, \quad (2)$$

and

$$|\Psi_T^f(z, \mathbf{r})|^2 = \frac{6\alpha_{em}}{4\pi^2} e_f^2 \{ [z^2 + (1-z)^2] \epsilon_f^2 K_1^2(\epsilon_f r) + m_f^2 K_0^2(\epsilon_f r) \}, \quad (3)$$

$$|\Psi_L^f(z, \mathbf{r})|^2 = \frac{6\alpha_{em}}{4\pi^2} e_f^2 [4Q^2 z^2 (1-z)^2 K_0^2(\epsilon_f r)], \quad (4)$$

with $(\epsilon_f^k)^2 = z_k(1-z_k)Q_k^2 + m_f^2$, $k = 1, 2$, e_f and m_f denote the charge and mass of the quark of flavor f and the functions K_0 and K_1 are the McDonald–Bessel functions. Moreover, $\sigma_{a,b}^{dd}(\bar{x}_{ab}, r_1, r_2)$ are the dipole-dipole total cross-sections corresponding to their different flavour content specified by the a and b indices. The variable \bar{x}_{ab} is given by:

$$\bar{x}_{ab} = \frac{Q_1^2 + Q_2^2 + 4m_a^2 + 4m_b^2}{W^2 + Q_1^2 + Q_2^2}, \quad (5)$$

which allows an extension of the model down to the limit $Q_{1,2}^2 = 0$. Note, that \bar{x}_{ab} depends on the flavour of scattering quarks.

Following [30] we will assume that

$$\sigma_{a,b}^{dd}(\bar{x}_{ab}, r_1, r_2) = \frac{2}{3} \sigma^{dp}(\bar{x}_{ab}, r_{\text{eff}}^2) \quad (6)$$

where σ^{dp} is the dipole - proton cross section and the effective radius is chosen to be [30]

$$r_{\text{eff}}^2 = \frac{r_1^2 r_2^2}{r_1^2 + r_2^2}. \quad (7)$$

For light flavours, equation (6) can be justified by the quark counting rule, as the ratio between the number of constituent quarks in a photon and the corresponding number of constituent quarks in the proton. We will assume that Eq. (6) is valid for all flavours. The dipole-proton cross section is given by:

$$\sigma^{dp}(x, \mathbf{r}) = 2 \int d^2\mathbf{b} \mathcal{N}(x, \mathbf{r}, \mathbf{b}), \quad (8)$$

where \mathcal{N} is the dipole-proton forward scattering amplitude for a given impact parameter \mathbf{b} which encodes all the information about the hadronic scattering, and thus about the non-linear and quantum effects in the hadron wave function. As usual we disregard the impact parameter dependence and assume that $\sigma^{dp} = \sigma_0 \mathcal{N}(x, \mathbf{r})$.

The forward scattering amplitude $\mathcal{N}(x, \mathbf{r})$ is a solution of the Balitsky-Kovchegov (BK) equation, which is given in leading order by

$$\frac{\partial \mathcal{N}(r, Y)}{\partial Y} = \int d\mathbf{r}_1 K^{\text{LO}}(\mathbf{r}, \mathbf{r}_1, \mathbf{r}_2) [\mathcal{N}(r_1, Y) + \mathcal{N}(r_2, Y) - \mathcal{N}(r, Y) - \mathcal{N}(r_1, Y)\mathcal{N}(r_2, Y)], \quad (9)$$

where $Y \equiv \ln(x_0/x)$ (x_0 is the value of x where the evolution starts), and $\mathbf{r}_2 = \mathbf{r} - \mathbf{r}_1$. K^{LO} is the evolution kernel, given by

$$K^{\text{LO}}(\mathbf{r}, \mathbf{r}_1, \mathbf{r}_2) = \frac{N_c \alpha_s}{2\pi^2} \frac{r^2}{r_1^2 r_2^2}, \quad (10)$$

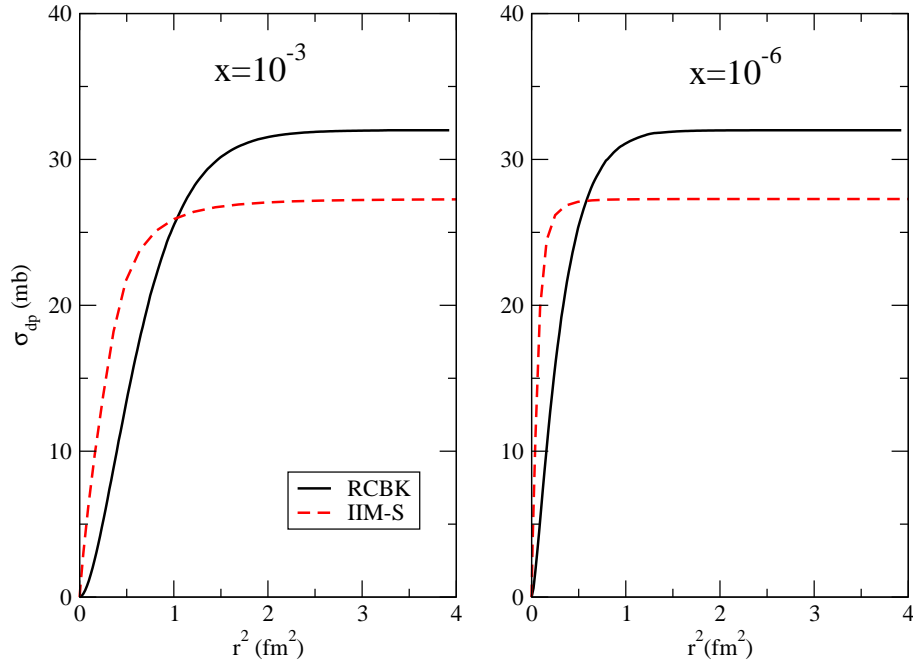


FIG. 2: Pair separation dependence of the rcBK (solid line) and IIM-S (dashed line) dipole cross sections at different values of x : (a) $x = 10^{-3}$ and (b) $x = 10^{-6}$.

where α_s is the strong coupling constant. This equation is a generalization of the linear BFKL equation (which corresponds of the first three terms), with the inclusion of the (non-linear) quadratic term, which damps the indefinite growth of the amplitude with energy predicted by BFKL evolution. The leading order BK equation presents some difficulties when applied to study DIS small- x data. In particular, some studies concerning this equation [33–37] have shown that the resulting saturation scale grows much faster with increasing energy ($\lambda \simeq 0.5$) than that extracted from phenomenology ($\lambda \simeq 0.2 - 0.3$). The calculation of the running coupling corrections to BK evolution kernel was explicitly performed in [5, 7], where the authors included $\alpha_s N_f$ corrections to the kernel to all orders. In [8] the improved BK equation was numerically solved replacing the leading order kernel in Eq. (9) by the modified kernel which includes the running coupling corrections and is given by [7]

$$K^{\text{Bal}}(\mathbf{r}, \mathbf{r}_1, \mathbf{r}_2) = \frac{N_c \alpha_s(r^2)}{2\pi^2} \left[\frac{r^2}{r_1^2 r_2^2} + \frac{1}{r_1^2} \left(\frac{\alpha_s(r_1^2)}{\alpha_s(r_2^2)} - 1 \right) + \frac{1}{r_2^2} \left(\frac{\alpha_s(r_2^2)}{\alpha_s(r_1^2)} - 1 \right) \right]. \quad (11)$$

Numerical studies of the improved BK equation [6] have confirmed that the running coupling corrections lead to a considerable slow-down of the evolution speed, which implies, for example, a slower growth of the saturation scale with energy, in contrast with the faster growth predicted by the LO BK equation. Since the improved BK equation has been shown to be quite successful when applied to the description of the ep HERA data for the proton structure function, we feel confident to use it in other physical situations such as $\gamma\gamma$ collisions. In what follows we make use of the public-use code available in [38].

The running coupling Balitsky - Kovchegov (rcBK) predictions will be compared with those from the parametrization proposed in Ref. [28], which was constructed so as to reproduce two limits of the LO BK equation analytically under control: the solution of the BFKL equation for small dipole sizes, $r \ll 1/Q_s(x)$, and the Levin-Tuchin law for larger ones, $r \gg 1/Q_s(x)$. In this parametrization, which generalizes the previous IIM parametrization [24], the heavy quark effects were estimated and the parametrization was updated including the fit of the new H1 and ZEUS data. In this parametrization the dipole-proton forward scattering amplitude is given by

$$\mathcal{N}(x, \mathbf{r}) = \begin{cases} \mathcal{N}_0 \left(\frac{r Q_s}{2} \right)^{2\left(\gamma_s + \frac{\ln(2/r Q_s)}{\kappa \lambda Y}\right)}, & \text{for } r Q_s(x) \leq 2, \\ 1 - \exp^{-a \ln^2(b r Q_s)}, & \text{for } r Q_s(x) > 2, \end{cases} \quad (12)$$

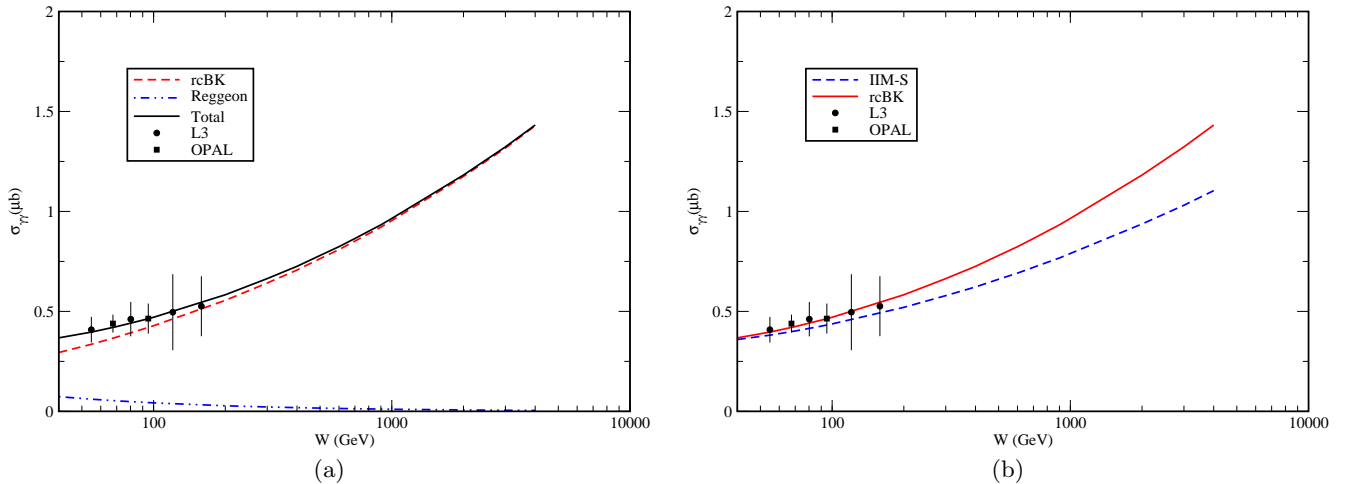


FIG. 3: (Color online) The total $\gamma\gamma$ cross section as a function of the energy W . (a) Contributions of the rcBK and Reggeon terms for the total cross sections. (b) Comparison between the rcBK and the IIM-S predictions.

where a and b are determined by continuity conditions at $rQ_s(x) = 2$, $\gamma_s = 0.7376$, $\kappa = 9.9$, $\lambda = 0.2197$, $Q_0^2 = 1.0$ GeV^2 , $x_0 = 0.1632 \times 10^{-4}$ and $\mathcal{N}_0 = 0.7$. Hereafter, we shall call the model above IIM-S. The first line from Eq. (12) describes the linear regime whereas the second one describes saturation effects.

In Fig. 2 we compare the pair separation dependence of rcBK and IIM-S dipole - proton cross sections at distinct values of x . The main differences between these models are the normalization of the cross sections and the rapid onset of saturation predicted by the IIM-S model. In comparison, the rcBK solution predicts a smooth growth, with a delayed saturation of the dipole cross section. Basically, the asymptotic saturation regime is only observed for very small values of x , beyond the kinematical range of HERA. The different normalizations is directly associated to the different values of σ_0 needed to describe the HERA data: $\sigma_0^{rcBK} = 31.6$ mb whereas $\sigma_0^{IIM} = 26.1$ mb. From the figure we can anticipate that the final $\gamma\gamma$ cross sections calculated with σ_{rcBK} will be larger than those calculated with σ_{IIM-S} and that the predicted energy dependence will be distinct.

Now we are ready to compute the two-photon cross section using the expression (1) with the standard photon wave function and with the two dipole cross sections discussed above. Following Ref. [30] we will consider in our calculations the following three cases of physical and phenomenological interest:

1. The case $Q_1^2 = Q_2^2 = 0$ corresponding to the interaction of two real photons.
2. The case $Q_1^2 \sim Q_2^2$ (with large $Q_{1,2}^2$) corresponding to the interaction of two (highly) virtual photons.
3. The case $Q_1^2 \gg Q_2^2$ corresponding to probing the structure of virtual ($Q_2^2 > 0$) or real ($Q_2^2 = 0$) photon at small values of the Bjorken parameter $x = Q_1^2/(2q_1q_2)$ ($Q_i^2 \equiv -q_i^2$). For instance, the structure function $F_2^\gamma(x, Q^2)$ of the real photon ($Q_2^2 = 0, Q_1^2 = Q^2$) is related in the following way to the $\gamma^*\gamma$ total cross-sections

$$F_2^\gamma(x, Q^2) = \frac{Q^2}{4\pi^2\alpha_{em}} [\sigma_{T,T}(W^2, Q^2, Q_2^2 = 0) + \sigma_{L,T}(W^2, Q^2, Q_2^2 = 0)]. \quad (13)$$

At this point a comment is in order. A shortcoming of the parametrization of the rcBK solution is that it is only valid at $x \leq 10^{-2}$. Consequently, we will focus our analysis in the energy range $W \geq 40$ GeV, restricting the comparison of our predictions with the experimental data in this kinematical range. In order to improve the description of the low energy data ($W < 100$ GeV), the inclusion of non-pomeron contributions was proposed in [30]. We follow the same approach and include a Reggeon contribution, which represents non-perturbative phenomena related to the Regge trajectories of light mesons, parametrized by

$$\sigma^R(W^2, Q_1^2, Q_2^2) = 4\pi^2\alpha_{em}^2 \frac{A_2}{a_2} \left[\frac{a_2}{(a_2 + Q_1^2)(a_2 + Q_2^2)} \right]^{1-\eta} \left(\frac{W^2}{a_2} \right)^{-\eta}. \quad (14)$$

The parameters A_2 , a_2 and η were obtained in [30] by fitting the experimental data. In what follows, we will use the same set of parameters: $A_2 = 0.26$, $a_2 = 0.2$ GeV^2 and $\eta = 0.3$. It is important to emphasize that this term is characterized by a decreasing energy and Q_i^2 dependence, which implies that its contribution is very small at $W > 30$

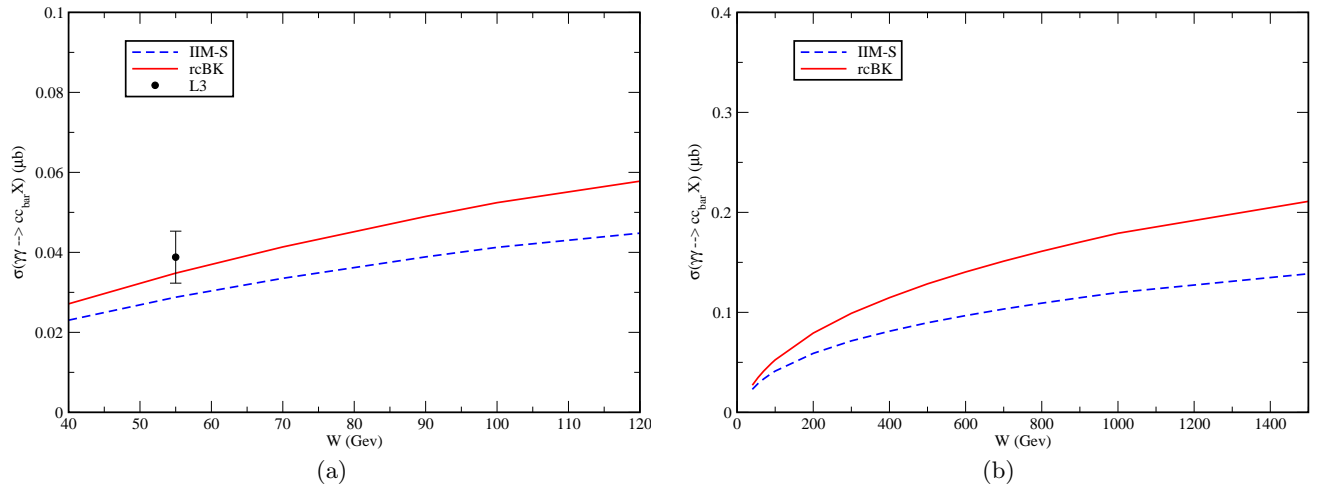


FIG. 4: (Color online) Charm production in $\gamma\gamma$ collisions. (a) Comparison between the rcBK and IIM-S predictions and the L3 data [41] at high energies. (b) Energy dependence of the charm cross section.

GeV. Moreover, the threshold corrections, which extend the applicability of the dipole approach up to larger values of x , are treated as in [30].

In Fig. 3 we plot $\sigma_{\gamma\gamma}$ as a function of the reaction energy W . In particular, in Fig. 3 (a) we present the rcBK prediction, the Reggeon term [Eq. (14)] and the sum of these two terms. As expected the Reggeon contribution can be disregarded at high energies. The experimental data [39, 40] are quite well described in our approach. In Fig. 3 (b) we compare the rcBK predictions with those from the IIM-S model. In both cases we are summing the same Reggeon term. Although both models describe the current experimental data, they predict very different values of the total cross sections at larger energies. This is directly associated to the rapid onset of saturation predicted by the IIM-S model, observed in Fig. 2. In what concerns the results presented in [30], we have found that the rcBK predictions are similar to those obtained using the GBW model.

Another important process which can be studied in the dipole approach is the heavy flavour production in $\gamma\gamma$ collisions. In this case it is assumed that one or the two dipoles is formed by heavy flavours and the distinct contributions are summed in the total heavy flavour cross section. Here we study the charm production assuming $m_c = 1.3$ GeV as in [30]. As the Reggeon exchange is associated to non-perturbative phenomena it is not included in our calculations of charm production, which is expected to be dominated by perturbative contributions. In Fig. 4 we present our predictions for the energy dependence of the charm cross section. In particular, in Fig. 4 (a) the rcBK and IIM-S predictions are compared with the L3 data [41] for $W > 40$ GeV. In contrast to the total $\gamma\gamma$ and γ^*p cross sections, which are described by these two models, the L3 data on charm production can only be well reproduced by the rcBK model. It is important to emphasize that the predictions obtained in [30] using a r_{eff} as given in Eq. (7) underestimate the experimental data. In Fig. 4 (b) we present our predictions for the charm cross section at the energy range of the future linear colliders. We observe that the predictions of the two models differ by about 75% at $W = 1$ TeV.

In Fig. 5 we present our predictions for the total $\gamma^*\gamma^*$ cross section for different photon virtualities. We assume that $Q_1^2 = Q_2^2 = Q^2$ and analyse the dependence of the cross section on the variable $Y \equiv \ln(W^2/Q_1Q_2)$. We can see that the cross sections increase with Y and decrease with Q^2 . Moreover, the rcBK and IIM-S predictions are similar at small Y but differ significantly at high Y . In particular, both predictions describe the experimental data [42] for $Q^2 = 20$ GeV². The rcBK model predicts large values of the total $\gamma^*\gamma^*$ cross section for high Y (high energies), which makes the experimental study of this observable feasible in future linear colliders.

Finally, in Fig. 6 we present our predictions for the x dependence of the photon structure function $F_2^\gamma(x, Q^2)$ for different values of the virtualities. The basic idea is that the quasi-real photon structure may be probed by other photon with a large momentum transfer. Moreover, we present in the panel (d) our predictions for the virtual photon structure function. Although there exist only very few data on this observable, its experimental study is feasible in future linear colliders. Our results predict that $F_2^\gamma(x, Q^2)$ increases at small- x , similarly to predictions for the proton structure function. The current experimental data [43] are described quite well. The rcBK and IIM-S predictions differ significantly at small- x , with the rcBK one predicting a steeper growth at small- x .

Lets summarize our main conclusions. In this paper we have estimated the main observables to be studied in $\gamma\gamma$ collisions in the future linear colliders. We have updated the predictions from Ref. [30] considering the state-of-the-art of the non-linear QCD dynamics, with the dipole scattering amplitude given by the solution of the running coupling

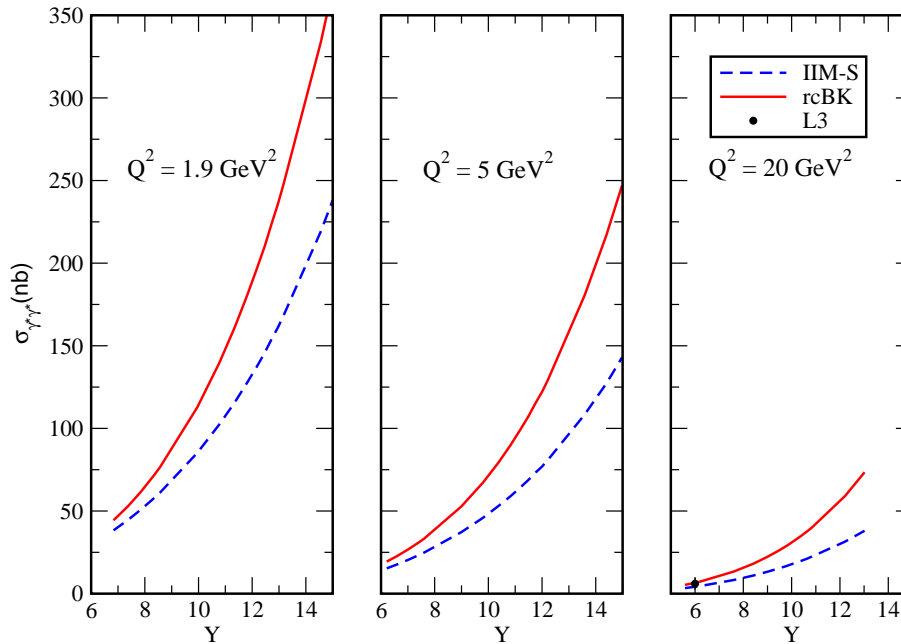


FIG. 5: The total $\gamma^*\gamma^*$ cross sections as a function of the variable $Y \equiv \ln(W^2/Q_1Q_2)$ for different values of Q^2 ($Q^2 = Q_1^2 = Q_2^2$).

Balitsky-Kovchegov equation. This allows us to obtain, for the first time, reliable estimates for these observables. In particular, our results agree with the current experimental data and demonstrate that the rcBK predictions are larger than those obtained using phenomenological models for higher energies. Moreover, our results show that the experimental study of $\gamma\gamma$ collisions can be useful to constrain the QCD dynamics.

Acknowledgments

This work was partially financed by the Brazilian funding agencies CNPq and FAPESP.

-
- [1] A. H. Mueller, Nucl. Phys. **B415**, 373 (1994); A. H. Mueller and B. Patel, Nucl. Phys. **B425**, 471 (1994); N. N. Nikolaev and B. G. Zakharov, Z. Phys. **C49**, 607 (1991); Z. Phys. **C53**, 331 (1992) .
- [2] L. N. Lipatov, Sov. J. Nucl. Phys. **23**, 338 (1976); E. A. Kuraev, L. N. Lipatov, V. S. Fadin, JETP **45**, 1999 (1977); I. I. Balitskii, L. N. Lipatov, Sov. J. Nucl. Phys. **28**, 822 (1978).
- [3] I. Balitsky, Nucl. Phys. B **463**, 99 (1996); Y. V. Kovchegov, Phys. Rev. D **60**, 034008 (1999); Phys. Rev. D **61**, 074018 (2000). L. D. McLerran and R. Venugopalan, Phys. Rev. D **49**, 2233 (1994); E. Iancu, A. Leonidov, L. McLerran, Nucl. Phys. A **692**, 583 (2001); E. Ferreiro, E. Iancu, A. Leonidov, L. McLerran, Nucl. Phys. A **703**, 489 (2002); J. Jalilian-Marian, A. Kovner, L. McLerran and H. Weigert, Phys. Rev. D **55**, 5414 (1997); J. Jalilian-Marian, A. Kovner and H. Weigert, Phys. Rev. D **59**, 014014 (1999), *ibid.* **59**, 014015 (1999), *ibid.* **59** 034007 (1999); A. Kovner, J. Guilherme Milhano and H. Weigert, Phys. Rev. D **62**, 114005 (2000); H. Weigert, Nucl. Phys. **A703**, 823 (2002).
- [4] F. Gelis, E. Iancu, J. Jalilian-Marian and R. Venugopalan, arXiv:1002.0333 [hep-ph]; E. Iancu and R. Venugopalan, arXiv:hep-ph/0303204; A. M. Stasto, Acta Phys. Polon. B **35**, 3069 (2004); H. Weigert, Prog. Part. Nucl. Phys. **55**, 461 (2005); J. Jalilian-Marian and Y. V. Kovchegov, Prog. Part. Nucl. Phys. **56**, 104 (2006).
- [5] Y. V. Kovchegov and H. Weigert, Nucl. Phys. A **784**, 188 (2007); Nucl. Phys. A **789**, 260 (2007); Y. V. Kovchegov, J. Kuokkanen, K. Rummukainen and H. Weigert, Nucl. Phys. A **823**, 47 (2009).
- [6] J. L. Albacete and Y. V. Kovchegov, Phys. Rev. D **75**, 125021 (2007).
- [7] I. Balitsky, Phys. Rev. D **75**, 014001 (2007); I. Balitsky and G. A. Chirilli, Phys. Rev. D **77**, 014019 (2008).

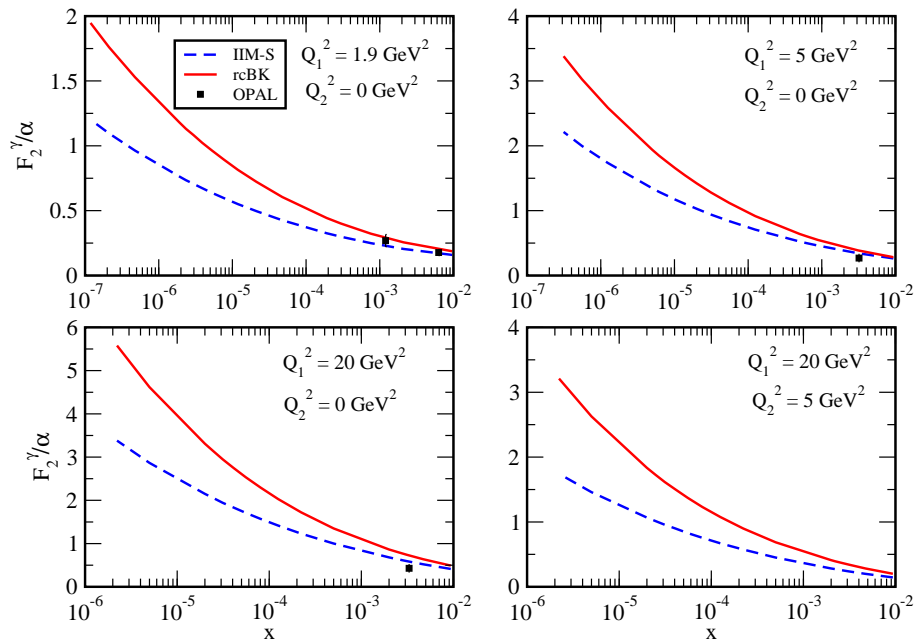


FIG. 6: The photon structure function $F_2^\gamma(x, Q^2)$ as a function of x for different choices of the virtualities Q_1^2 and Q_2^2 .

- [8] J. L. Albacete, N. Armesto, J. G. Milhano and C. A. Salgado, Phys. Rev. **D80**, 034031 (2009).
- [9] H. Weigert, J. Kuokkanen and K. Rummukainen, AIP Conf. Proc. **1105**, 394 (2009).
- [10] M. A. Betemps, V. P. Goncalves and J. T. de Santana Amaral, Eur. Phys. J. C **66**, 137 (2010).
- [11] V. P. Goncalves, M. V. T. Machado and A. R. Meneses, Eur. Phys. J. C **68**, 133 (2010).
- [12] J. L. Albacete and C. Marquet, Phys. Lett. B **687**, 174 (2010).
- [13] R. Nisius, Phys. Rept. **332**, 165 (2000).
- [14] J. Bartels, A. De Roeck, H. Lotter, Phys. Lett. B **389**, 742 (1996); J. Bartels, C. Ewerz, R. Staritzbichler, Phys. Lett. B **492**, 56 (2000); A. Bialas, W. Czyz, W. Florkowski, Eur. Phys. J. C **2**, 683 (1998); J. Kwiecinski, L. Motyka, Eur. Phys. J. C **18**, 343 (2000); N. N. Nikolaev, B. G. Zakharov, V. R. Zoller, JETP **93**, 957 (2001); S. J. Brodsky, F. Hautmann, D. E. Soper, Phys. Rev. D **56**, 6957 (1997); Phys. Rev. Lett. **78**, 803 (1997).
- [15] M. Boonekamp, A. De Roeck, C. Royon, S. Wallon, Nuc. Phys. B **555**, 540 (1999).
- [16] S.J. Brodsky, V.S. Fadin, V.T. Kim, L.N. Lipatov, G.B. Pivovarov, Pis'ma ZHETF **76**, 306 (2002) [JETP Letters **76**, 249 (2002)].
- [17] V. P. Goncalves, M. V. T. Machado and W. K. Sauter, J. Phys. G **34** (2007) 1673
- [18] F. Caporale, D. Y. Ivanov and A. Papa, Eur. Phys. J. C **58** (2008) 1
- [19] K. Golec-Biernat and M. Wüsthoff, Phys. Rev. D **60**, 114023 (1999); Phys. Rev. D **59**, 014017 (1998).
- [20] J. Bartels, K. Golec-Biernat and H. Kowalski, Phys. Rev. D **66** (2002) 014001.
- [21] H. Kowalski and D. Teaney, Phys. Rev. D **68**, 114005 (2003).
- [22] H. Kowalski, L. Motyka and G. Watt, Phys. Rev. D **74**, 074016 (2006).
- [23] D. Kharzeev, Y.V. Kovchegov and K. Tuchin, Phys. Lett. **B599**, 23 (2004).
- [24] E. Iancu, K. Itakura, S. Munier, Phys. Lett. B **590**, 199 (2004).
- [25] A. Dumitru, A. Hayashigaki and J. Jalilian-Marian, Nucl. Phys. **A765**, 464 (2006); Nucl. Phys. **A770**, 57 (2006).
- [26] V. P. Goncalves, M. S. Kugeratski, M. V. T. Machado and F. S. Navarra, Phys. Lett. B **643**, 273 (2006).
- [27] D. Boer, A. Utermann and E. Wessels, Phys. Rev. D **77**, 054014 (2008).
- [28] G. Soyez, Phys. Lett. B **655**, 32 (2007).
- [29] G. Watt and H. Kowalski, Phys. Rev. D **78**, 014016 (2008).
- [30] N. Timneanu, J. Kwiecinski, L. Motyka, Eur. Phys. J. C **23**, 513 (2002).
- [31] N. N. Nikolaev, J. Speth and V. R. Zoller, Eur. Phys. J. C **22**, 637 (2002); J. Exp. Theor. Phys. **93**, 957 (2001) [Zh. Eksp. Teor. Fiz. **93**, 1104 (2001)].
- [32] A. Donnachie, H. G. Dosch and M. Rueter, Phys. Rev. D **59**, 074011 (1999).
- [33] E. Iancu, K. Itakura and L. McLerran, Nucl. Phys **A708**, 327 (2002).
- [34] A. H. Mueller and D. N. Triantafyllopoulos, Nucl. Phys. **B640**, 331 (2002).

- [35] N. Armesto and M. A. Braun, Eur. Phys. J. **C20**, 517 (2001).
- [36] M. A. Braun, Phys. Lett. B **576**, 115 (2003).
- [37] J. L. Albacete, N. Armesto, J. G. Milhano, C. A. Salgado, and U. A. Wiedemann, Phys. Rev. D **71**, 014003 (2005).
- [38] <http://www-fp.usc.es/phenom/rcbk>
- [39] G. Abbiendi *et al.* [OPAL Collaboration], Eur. Phys. J. C **14** (2000) 199
- [40] M. Acciarri *et al.* [L3 Collaboration], Phys. Lett. B **519** (2001) 33
- [41] M. Acciarri *et al.* [L3 Collaboration], Phys. Lett. B **514** (2001) 19
- [42] M. Acciarri *et al.* [L3 Collaboration], Phys. Lett. B **453** (1999) 333.
- [43] M. Acciarri *et al.* [L3 Collaboration], Phys. Lett. B **447** (1999) 147; G. Abbiendi *et al.* [OPAL Collaboration], Eur. Phys. J. C **18** (2000) 15.